A Modeling Framework for System Restoration from Cascading Failures

Chaoran Li, Daqing Li, Enrico Zio, Rui Kang, Zhen Wang

HAL Id: hal-01787044
https://hal.science/hal-01787044

Submitted on 13 Jul 2020

RESEARCH ARTICLE

A Modeling Framework for System Restoration from Cascading Failures

Chaoran Liu[1,2], Daqing Li[1,2]*, Enrico Zio[3,4]*, Rui Kang[1,2]

1. School of Reliability and Systems Engineering, Beihang University, Beijing, China, **2.** Science and Technology on Reliability and Environmental Engineering Laboratory, Beijing, China, **3.** Chair on Systems Science and the Energetic challenge, European Foundation for New Energy-Electricite' de France, Ecole Centrale Paris and Supelec, Paris, France, **4.** Dipartimento di Energia, Politecnico di Milano, Milano, Italy

*li.daqing.biu@gmail.com (DL); enrico.zio@ecp.fr (EZ)

Abstract

System restoration from cascading failures is an integral part of the overall defense against catastrophic breakdown in networked critical infrastructures. From the outbreak of cascading failures to the system complete breakdown, actions can be taken to prevent failure propagation through the entire network. While most analysis efforts have been carried out before or after cascading failures, restoration during cascading failures has been rarely studied. In this paper, we present a modeling framework to investigate the effects of in-process restoration, which depends strongly on the timing and strength of the restoration actions. Furthermore, in the model we also consider additional disturbances to the system due to restoration actions themselves. We demonstrate that the effect of restoration is also influenced by the combination of system loading level and restoration disturbance. Our modeling framework will help to provide insights on practical restoration from cascading failures and guide improvements of reliability and resilience of actual network systems.

Introduction

Cascading failure is a common mechanism of large-scale failures in complex network systems, such as electric power transmission grids, water/gas delivery systems, railways, etc. [1–7]. For a practical example, we can refer to the large-scale blackouts of electric power transmission systems resulting from cascading failures initiated by component overloads [6, 8]. Occurrences of cascading failures are found statistically more significant than that expected by theory [6, 9]. Given the vital societal importance of these critical infrastructures, there is a strong interest in the studies for the design, implementation and evaluation of effective

restoration strategies against cascading failures, which rescue systems from the brink of collapse and avoid the amplification of their consequences [10–13].

Efforts have been carried out to study how to reduce the frequency, duration, intensity and extent of cascading failures. There are many design measures to avoid cascading failures, such as robust structures [14–19], capacity and structural redundancy design [19–22] and n-1 criterion [23], by which cascading failures can hardly be eliminated [24]. After the failure cascades, black-start [25, 26], system reconfiguration [27, 28] and corrective restoration [29, 30] are used to bring the system back to its normal operation conditions.

While complete prevention against cascading failures in design stage proves impossible and post-actions only passively recover systems at a large cost, active in-process restoration can mitigate cascading failure during its evolution, leading the system to a stable state. The primary objective of restoration during the process of cascading failures is to take actions to prevent failures from unfolding to catastrophic failures and eventually to minimize the damage, e.g. minimizing the unserved loads in an electric power transmission grid. For example, references [31, 32] propose three different strategies based on line switching to minimize the consequences of cascading failures on the entire system, on predetermined areas of the system or on both within a multi-objective optimization framework. References [33–36] introduce and analyze some restoration planning and restoration actions. Based on the development of fast recovery technology [37], it is possible to mitigate and rescue the system from the cascading failures through real time restoration of network components. Going back to the example of the electric power transmission grid, restoration against cascading failures may be achieved in practice through real-time controlled islanding [38, 39], selective load shedding [38, 39], wide area monitoring [40], real-time fault analysis and validating relay operations [41], etc.

In this paper, we present a novel modeling framework for analyzing restoration in network systems subject to cascading failures. The framework is used to study the effects of different restoration strategies in terms of restoration timing and strength: t_r, the restoration timing in the process of the cascading failure, and p_r, the restoration strength, which is quantified by the probability of repairing a failed component. Repair here means full, immediate recovery which can be realized in practice by utilizing fast recovery technology. We study how different restoration strategies described in terms of the two basic quantities (t_r and p_r) influence the overall system reliability.

Description of the Restoration Model

We first consider an unweighted and fully connected network of N identical components [42]. The loading-dependent model proposed in [43] is adopted to describe the dynamics of cascading failures. The model is analytically tractable and captures some essential features of the cascading failure process, which helps to understand the mechanism of failure propagation in the network system. The

model describes a network composed of identical components with load distributed uniformly in $[L_{min}, L_{max}]$, and the average initial component loading $L=(L_{min}+L_{max})/2$. An initial disturbance D is added to all components, and may cause some components to exceed their capacity threshold $L_{fail}=1$, which is assumed identical for all the components. If component j is working and $L_j+D>L_{fail}$, component j fails. Then, each failure of a component leads to an additional load $P>0$ added to all the other functional components in the network, which may cause further failures in a cascade.

The restoration actions will be considered once the cascading failures process has been triggered. A typical in-process restoration procedure is comprised of three stages [33, 34]: firstly, estimating system/component status, locating the critical loads, and developing the strategies for rebuilding the network connections; secondly, identifying the paths of restoration, energizing and interconnecting subsystems; thirdly, restoring most of lost loads. Restoration strategies differ from each other in the above aspects. Here we propose a restoration model considering the timing and strength of restoration, which mainly determine the effects of restoration. In the model, each failed component is repaired with a certain probability p_r at a given step $t_r>0$ during cascading failure. The restoration actions recover the links of the component to be repaired, while its links to failed components remain disconnected. We assume that restoration may cause some disturbance to the existing functional components in the network. We model this restoration disturbance by adding a random perturbation D_r distributed uniformly in $[D_r^{min}, D_r^{max}]$ to the load of each functional component. The value of restoration disturbance depends on whether the restoration action is implemented appropriately to the system, which could be positive or negative. This means that the restoration may either reduce or increase the loads of the functional components, depending on whether it is beneficial or harmful.

The following algorithm is used to realize the above procedure. The details of the algorithm are summarized as follows:

1. All N components are initially functional and loaded by quantities L_1, L_2, …, L_n, which are independent random variables uniformly distributed in $[L_{min}, L_{max}]$. Initialize the stage counter t to zero.
2. Add the initial disturbance load D to the load of each component: then, the load of component j is L_j+D.
3. Each existing component is examined: if the current load of component j is larger than L_{fail}, component j fails. We denote the number of components failed in this single step by M_t. Add M_tP to the load of each functional component. The stage counter t is incremented by one.
4. When t reaches the restoration moment tr, i.e., $t=tr$, each failed component is repaired with probability pr by reconnecting it to its adjacent functional components. The load of each repaired component is reassigned uniformly in $[L_{min}, L_{max}]$. Add a random disturbance Dr uniformly distributed in $[D_r^{min}, D_r^{max}]$ to the load of each functional component.

5. Go back to step 3, unless the cascading failures stop.

Effects of Restoration Strategies

In this section, we study the effects of different restoration strategies on the system robustness against cascading failures and the resulting system reliability. We begin our study by evaluating the restoration effect on the total damage made by cascading failure (the average avalanche size). Figure 1 compares different restoration strategies in terms of restoration timing t_r and strength p_r by measuring the number of failed components ES. As shown in [44], there is a transition of ES occurring at critical point L_c=0.8 without restoration (p_r=0). When the value of L is below this threshold, few failures emerge. On the other hand, for L above the threshold, there is a significant risk of cascading failures that lead to global collapse of the system. And in-process restoration can reduce the final damage significantly if it is implemented properly. As shown in Fig. 1, cascading failure under restoration (p_r>0) with negative D_r generates much smaller avalanche size ES than the case without restoration (p_r=0). Furthermore, for negative D_r, early restoration (e.g., t_r=1) ends up with more functional components than late restoration (e.g., t_r=4). For positive D_r, restoration worsens the system in terms of ES.

To investigate the effects of different restoration strategies on improving the reliability against cascading failures, we measure the system load fluctuations (SLF) defined as

$$SLF = \sum_{i=1}^{T} |SL(t=i) - SL(t=0)|, \tag{1}$$

where

$$SL(t=i) = \sum_{j=1}^{N} L_j(t=i). \tag{2}$$

N is the total number of the components in the network system. L_j is the load of component j, and we set $L_j(t=i) = 0$ if component j is failed at the moment i. $SL(t=0)$ is the initial system load when the system maintains its normal functional state. $SL(t=i)$ is the total load of system at the moment i in the cascading process, i.e., the sum of the loads of all functional components. The parameter T is the duration of the whole dynamical process of cascading failures.

The measure SLF reflects the system instability in the whole process of cascading failures, considering the required balance between the supply and demand. Figure 2 shows SLF under restoration at a given restoration timing t_r as a function of the restoration probability p_r. From Figs. 2a–2d, we can see that the restoration with negative disturbance can effectively mitigate cascading failures and reduce system instability. Furthermore, the system can be improved by high strength of restoration.
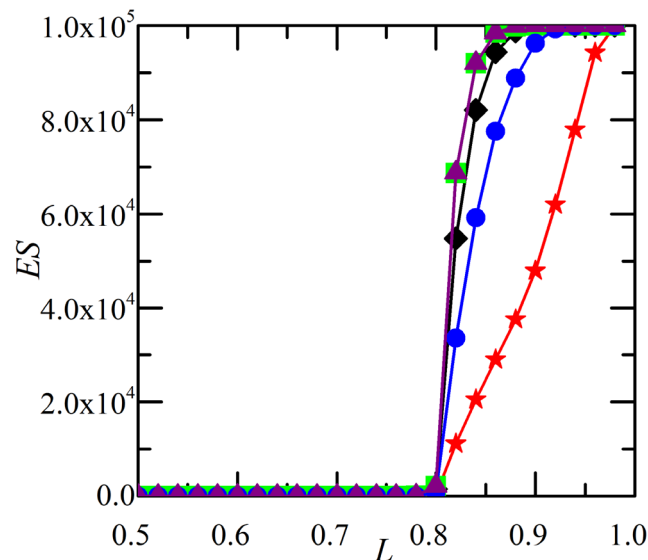
Figure 1. Average avalanche size *ES* as a function of the system loading level *L*. Results for five different restoration strategies: (1) p_r=0 (black diamonds); (2) t_r=1, p_r=1, D_r^{min}=6 × 10^{-6}, D_r^{max}=8 × 10^{-6} (green squares); (3) t_r=4, p_r=1, D_r^{min}= 6 × 10^{-6}, D_r^{max}=8 × 10^{-6} (purple triangles); (4) t_r=1, p_r=1, D_r^{min}=−8 × 10^{-6}, D_r^{max}=−6 × 10^{-6} (red stars); (5) t_r=4, p_r=1, D_r^{min}=−8 × 10^{-6}, D_r^{max}=−6 × 10^{-6} (blue circles). Each curve corresponds to the average over twenty thousand realizations of networks with 10^5 components. The example network system has no specific topology, on which the results do not depend. The initial component loading can vary from L_{min} to L_{max}=L_{fail}=1. Then, L=(L_{min}+1)/2 may be increased by increasing L_{min}. The initial disturbance $D = 4 × 10^{-6}$ is assumed to be the same as the load transfer amount P=4 × 10^{-6}. All the investigated network systems without restoration satisfy the cascading condition that the cascade step is no less than 5.

doi:10.1371/journal.pone.0112363.g001
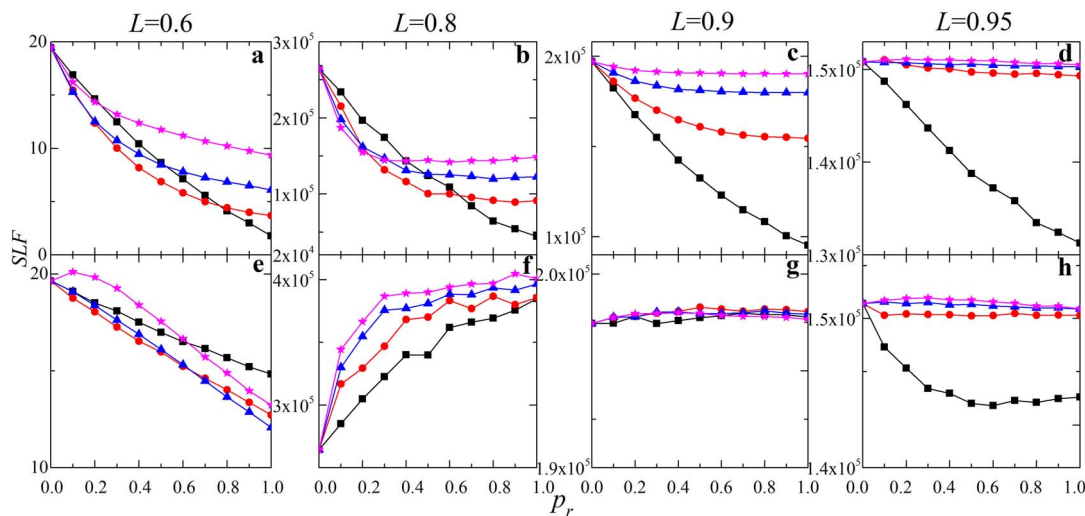
Figure 2. System load fluctuations *SLF* as a function of restoration probability p_r for different system loading level *L*. According to the proposed modeling framework for restoration, we compare different strategies in four cases of t_r=1 (black squares), t_r=2 (red circles), t_r=3 (blue triangles), t_r=4 (magenta stars). D_r^{min}=−8 × 10^{-6}, D_r^{max}=−6 × 10^{-6} for the panel above, and D_r^{min}=6 × 10^{-6}, D_r^{max}=8 × 10^{-6} for the panel below. The other parameters are the same as in Fig. 1.

doi:10.1371/journal.pone.0112363.g002

The situation for positive restoration disturbance is more surprising. One may expect that restoration would worsen the cascading failure when D_r is positive. The corresponding results with positive D_r are complicated: restoration can still improve the system for subcritical loading (Fig. 2e); at critical loading L_c, restoration produces quite large SLF and induces extra instability (Fig. 2f); for supercritical loading, restoration has almost no impact on SLF (e.g., $L=0.9$, Fig. 2g).

The results above can be explained as follows. The restoration effect is dominated by two factors, restored components and the consequential restoration disturbance. These two factors are cooperative under negative D_r so that failed components are recovered, when the load of functional components is decreased. This cooperative effect under negative D_r can be stronger for early restoration. When D_r is positive, however, restoration will increase the load of functional components when failed components are restored at the same time. The outcome of restoration then depends on the competition between these two factors.

To further explore the effect of restoration disturbance, in Fig. 3 we analyze the restoration effect as a function of the restoration disturbance. For $L=0.6$ and 0.8, restoration ($p_r=1$) significantly increases SLF as the restoration disturbance increases (Figs. 3a and 3b). For supercritical loading, SLF increases for negative D_r and then remains saturated for positive D_r ($L=0.9$, Fig. 3c), while early restoration ($t_r=1$) can improve system for both negative and positive D_r ($L=0.95$, Fig. 3d). Similar as the results in Fig. 2, restoration under negative D_r at an early cascade step is beneficial for all investigated cases. When restoration disturbance D_r is positive, restoration improves system only for certain values of system loading.

To observe the dynamical processes of restoration, we track the system evolution under restoration in terms of system fluctuations during cascading failure. The load fluctuation of the system at the moment t is defined as

$$LF(t=i) = |SL(t=i) - SL(t=0)|. \tag{3}$$

For convenience, here we assume that $LF(t)=0$ when $t>T$. Figure 4 demonstrates the system evolution process in terms of load fluctuation $LF(t)$, where total system load fluctuation is the corresponding area under the curve of $LF(t)$. Early restoration ($t_r=1$) under negative D_r is shown to reduce the load fluctuation since the restoration moment in the process of cascading failures (Figs. 4a–4d). However, for positive D_r, load fluctuation of restoration at $L=0.6$ is lower than that without restoration (Fig. 4e), while for $L=0.8$ load fluctuation is significantly increased (Fig. 4f). And it is not helpful to restore system late with positive D_r for a system high loaded (Figs. 4g and 4h).

Analytical Methods

According to the proposed restoration model, n components are loaded in $[L_{\min}, L_{\max}]$. We set $=(L_{\min}+L_{\max})/2$ and $L_{\max}=L_{\text{fail}}=1$. Then component j has the load
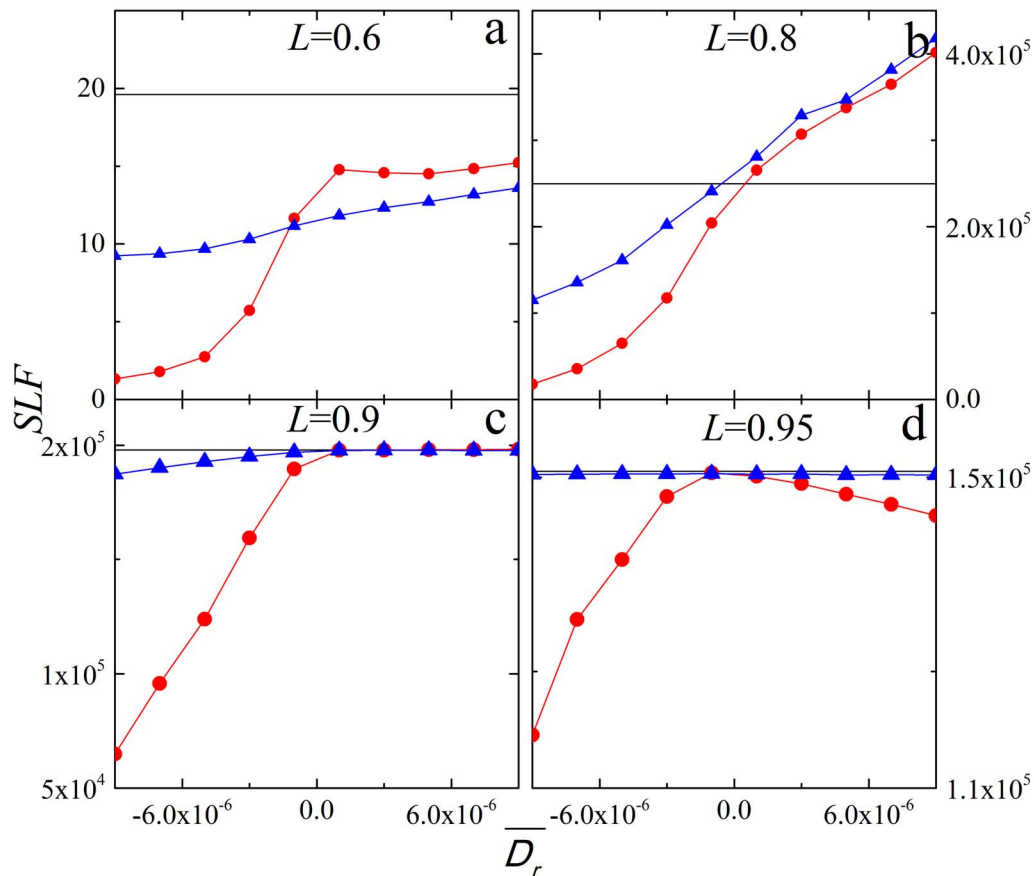
Figure 3. System load fluctuations *SLF* as a function of the average restoration disturbance $\overline{D_r} = (D_r^{\min} + D_r^{\max})/2$ for different system loading level *L*. Results for different restoration strategies: (1) $p_r=0$ (black, straight line); (2) $t_r=1$, $p_r=1$ (red circles); (3) $t_r=4$, $p_r=1$ (blue triangles). Here we set $D_r^{\max} - D_r^{\min} = 2 \times 10^{-6}$. The other parameters are the same as in Fig. 1. Notice that *SLF* in case of $p_r=0$ remains constant as *SLF* is independent of D_r without restoration.

$L_j \in [2L-1, 1]$ and fails when its load is larger than L_{fail}. An initial disturbance D is added to each component. Each failed component transfers a fixed amount of load P to other functional components.

Based on the literature [44], the distribution of the total number of failed components S without restoration can be given by

$$P(S=r) = \begin{cases} \dbinom{n}{r} d(d+rp)^{r-1}(1-d-rp)^{n-r}, & r=0,1,\cdots,\left[\dfrac{1-d}{p}\right] \\ 0, & r=\left[\dfrac{1-d}{p}\right]+1,\cdots,n-1 \quad (4) \\ 1-\displaystyle\sum_{s=0}^{n-1} P(S=s), & r=n, \end{cases}$$

where, $[x]$ is the largest integer not more than x and $0 \le d = \dfrac{D}{2-2L} \le 1$, $p = \dfrac{P}{2-2L} > 0$, $\left[\dfrac{1-d}{p}\right] < n$.
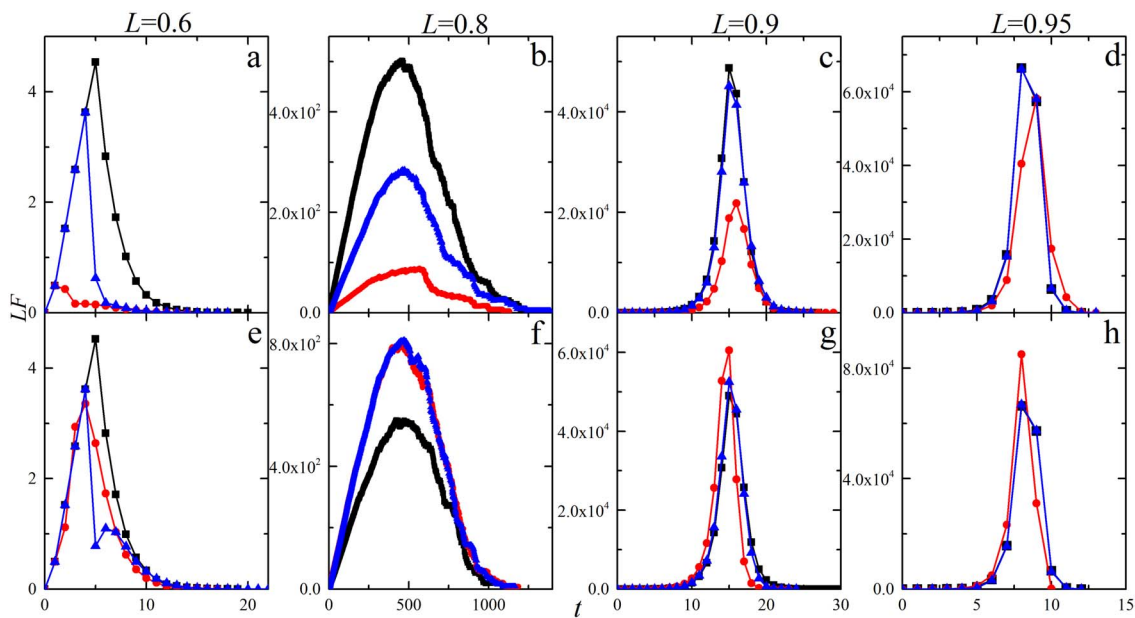
Figure 4. Load fluctuations *LF*(*t*) during cascading failures. Results for different restoration strategies: $p_r = 0$ (black squares), $t_r = 1$, $p_r = 1$ (red circles) and $t_r = 4$, $p_r = 1$ (blue triangles). Here, the *x* axis is the system unstable moment *t* based on cascade and restoration. $D_r^{\min} = -8 \times 10^{-6}$, $D_r^{\max} = -6 \times 10^{-6}$ for the panel above and $D_r^{\min} = 6 \times 10^{-6}$, $D_r^{\max} = 8 \times 10^{-6}$ for the panel below. The other parameters are the same as in Fig. 1.

doi:10.1371/journal.pone.0112363.g004

When $rp + d \leq 1$, $n \to \infty$, $p \to 0$, $d \to 0$, $\theta = nd$, $\lambda = np$, the above distribution can be approximated by a branching process with

$$P(S = r) \approx \theta(r\lambda + \theta)^{r-1} \frac{e^{-r\lambda - \theta}}{r!}. \tag{5}$$

Then we have the approximation [45] based on the property of this branching process

$$P(M_1 = m_1) = \begin{cases} e^{-\theta} \dfrac{\theta^{m_1}}{m_1!}, & m_1 = 0, 1, \cdots, n-1 \\ 1 - e^{-\theta} \displaystyle\sum_{k=0}^{n-1} \dfrac{\theta^k}{k!}, & m_1 = n, \end{cases} \tag{6}$$

and

$$
\begin{aligned}
&P(M_{i+1} = m_{i+1} | M_i = m_i, \cdots, M_1 = m_1) \\
&= \begin{cases} \dfrac{(m_i\lambda)^{m_{i+1}}}{m_{i+1}!} e^{-m_i\lambda}, & m_{i+1} = 0, 1, \cdots, n - s_i - 1 \\ 1 - \displaystyle\sum_{k=0}^{n-s_i-1} \dfrac{(m_i\lambda)^k}{k!} e^{-m_i\lambda}, & m_{i+1} = n - s_i, \end{cases}
\end{aligned} \tag{7}
$$

Where $s_i = m_1 + \cdots + m_i$.

As our investigated configurations satisfy the cascading condition that the cascade step is no less than 5 (or any arbitrary number), we obtain $P(T \geq 5) = P(M_5 \neq 0) = 1 - P(M_5 = 0) = p(\theta, \lambda)$. Then the distribution of the total number of failed components S without restoration ($p_r = 0$) is

$$
\begin{aligned}
P(S = r | M_5 \neq 0) &= \frac{P(S = r, M_5 \neq 0)}{P(M_5 \neq 0)} \\
&= \frac{P(S = r) - P(S = r, M_5 = 0)}{P(M_5 \neq 0)} \approx \frac{P(S = r)}{P(M_5 \neq 0)} (5 \leq r < n).
\end{aligned}
$$
(8)

According the parameters in the text, we set $\lambda = np = \dfrac{nP}{2 - 2L_c} = 1$ and get the critical loading $L_c = 0.8$, which corresponds to the case in [Fig. 1](#).

When the restoration strategy (t_r, p_r) $(t_r > 0, p_r > 0)$ is taken, we assume that the total number of components failed at restoration timing is $S_{t_r} = s_{t_r} < n$. Then the current state of the system is as follows: m failed components, $s_{t_r} - m$ restored components loaded in $[2L - 1, 1]$, $(n - s_{t_r})$ functional components loaded in $[2L - 1 + D + s_{t_r}P + D_r, 1 + M_{t_r}P + D_r]$, and the failed rate is $\dfrac{M_{t_r}P + D_r}{2 - 2L - D - s_{t_{r-1}}P}$, $Em = (1 - p_r)s_{t_r}$. Then the system may go on evolving after the restoration. And we can clearly know the average avalanche size ES is strongly dependent on the value and sign symbol of the restoration disturbance D_r, the restoration timing t_r, the restoration strength p_r and the system loading level L.

When $M_{t_r}P + D_r \leq 0$, restoration ends the cascading failure. Then the distribution of the total number of components failed S with restoration is

$$
P(S = s_r | M_5 \neq 0) = \sum_{r_1 = s_r}^{n} P(S_{t_r} = r_1 | M_5 \neq 0) C_{r_1}^{s_r} (1 - p_r)^{s_r} p_r^{r_1 - s_r} (0 \leq s_r < n). \quad (9)
$$

When $M_{t_r}P + D_r > 0$, the state of system at t_r can be replaced by m failed components and $(n - m)$ functional components loaded in $[2L - 1, 1]$ disturbed by the load $D' = \dfrac{(D + s_{t_r}P + M_{t_r}P + 2D_r)(n - s_{t_r})}{2(n - m)}$. Considering the cascading condition that the cascade step is no less than 5 (or any arbitrary number) and the restoration timing t_r, the distribution of the total number of components failed S with restoration is
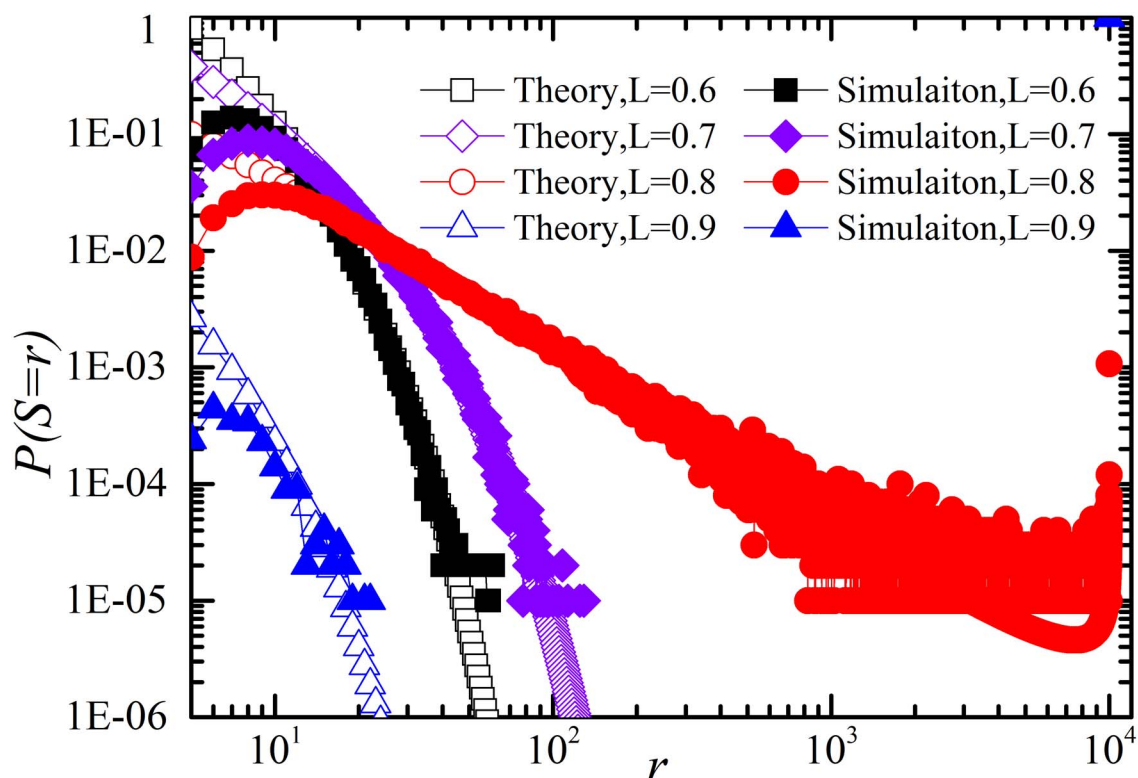
Figure 5. Log-log plot of distribution of number of components failed S for different system loading level L without restoration (p_r=0). Note the power-law region for the critical loading L=0.8. Simulation results are averaged over 100,000 realizations of the systems. The related parameters are N=10000, D=P=0.00004. Note that the simulation results coincide well with theoretic analysis.

$$P(S=r|M_5 \neq 0)$$

$$= \sum_{r_1=0}^{n} P(m=r_1|M_5 \neq 0)P(S=r|m=r_1)$$

$$= \sum_{r_2=1}^{n} \sum_{r_1=0}^{r_2} P(S_{tr}=r_2|M_5 \neq 0)C_{r_2}^{r_1}(1-p_r)^{r_1}p_r^{r_2-r_1}P_1(S_r=r-r_1) \qquad (10)$$

$$\approx \sum_{r_2=1}^{n} \sum_{r_2=m_1+\cdots+m_{tr},m_i>0} \sum_{r_1=0}^{r_2} \frac{P(M_1=m_1,\cdots,M_{tr}=m_{tr})}{P(M_5 \neq 0)}C_{r_2}^{r_1}(1-p_r)^{r_1}p_r^{r_2-r_1}P_1(S_r=r-r_1)(5<r<n')$$

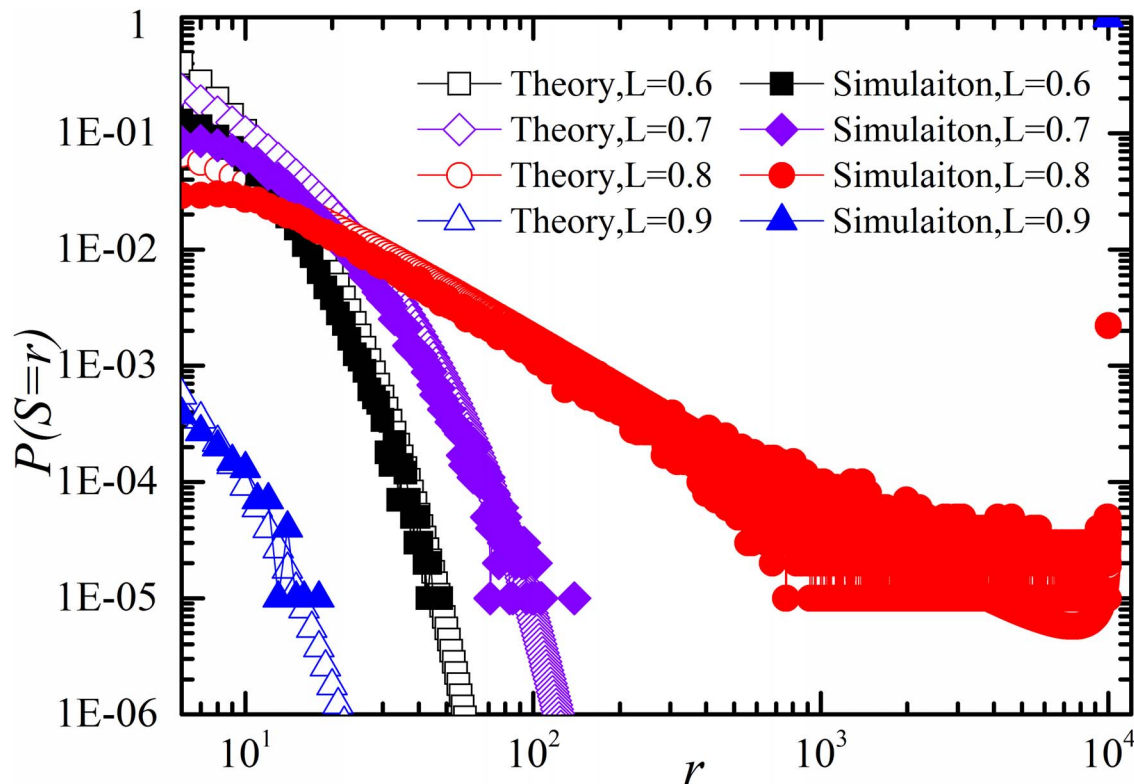And the distribution of the total number of components failed S_r after restoration is

Figure 6. Log-log plot of distribution of number of components failed S for different system loading level L with restoration (t_r=1, p_r=1). $D_r^{min} = D_r^{max} = -4 \times 10^{-6}$ and the other parameters are the same as in Fig. 5. Note that the simulation results coincide well with theoretic analysis.

doi:10.1371/journal.pone.0112363.g006

$$P_1(S_r = r) = \begin{cases} \binom{n'}{r} d'(d'+rp)^{r-1}(1-d'-rp)^{n'-r}, & r = 0, \cdots, \left[\dfrac{1-d'}{p}\right] \\ 0, & r = \left[\dfrac{1-d'}{p}\right] + 1, \cdots, n'-1 \quad (11) \\ 1 - \sum_{s=0}^{n'-1} P_1(S_r = s), & r = n'. \end{cases}$$

where $n' = n - m$, $d' = \dfrac{D'}{2-2L}$, $p = \dfrac{P}{2-2L}$.

Next we give the analytical results for the proposed modeling framework of restoration. Firstly, we give the comparison between the simulation and theory in case of p_r=0 in Fig. 5. The case corresponds to Eq. (8). As shown in Fig. 5, theoretical calculation coincides well with the numerical simulations. And the distribution behaves as a power-law at the critical loading, at which system has a high probability of large-scale failures.

Then, we give the comparison of restoration between simulation and theory in Fig. 6 for negative D_r and Fig. 7 for positive D_r in case of $p_r \neq 0$. These cases
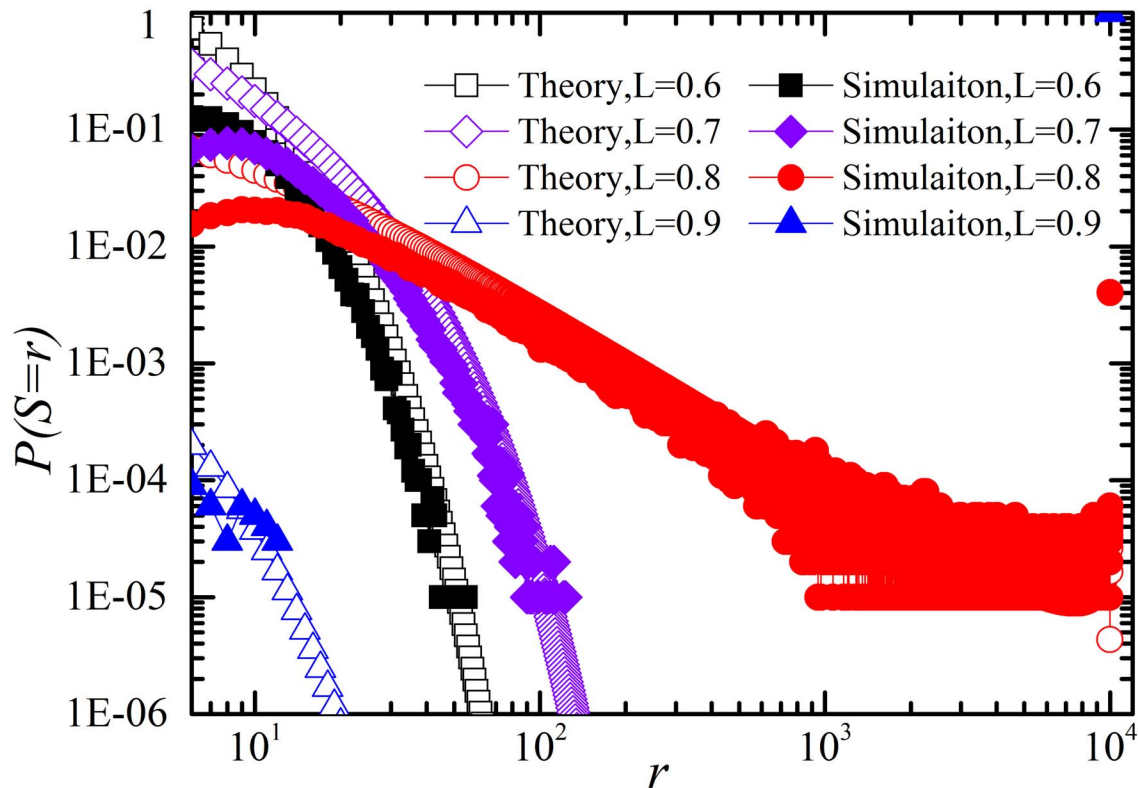
Figure 7. Log-log plot of distribution of number of components failed *S* for different system loading level *L* with restoration (t_r=1, p_r=1).
$D_r^{\min} = D_r^{\max} = 4 \times 10^{-5}$ and the other parameters are the same as in Fig. 5. Note that the simulation results coincide well with theoretic analysis.

doi:10.1371/journal.pone.0112363.g007

correspond to Eq. (10). As shown in Fig. 6 and Fig. 7, theoretical calculation coincides well with the numerical simulations.

Model Variations

We apply our modeling framework of restoration to the western U.S. power transmission grid [46] for the model validation. Here we present the results in Fig. 8 and Fig. 9 on the realistic power system with more practical consideration in the model:

Variation 1: initial load distribution. We change the distribution of initial component loading from uniform distribution to Gaussian distribution;

Variation 2: impact of each failed component on the functional components. Previously, each failure of a component leads to an additional load $P>0$ added to all the other functional components in the network regardless of network topology. Now each failed component leads to an additional load $Q>0$ only added to its functional neighbors, which is dependent on network topology;

Variation 3: restoration disturbance D_r. We change the distribution of restoration disturbance from uniform distribution to Gaussian distribution.
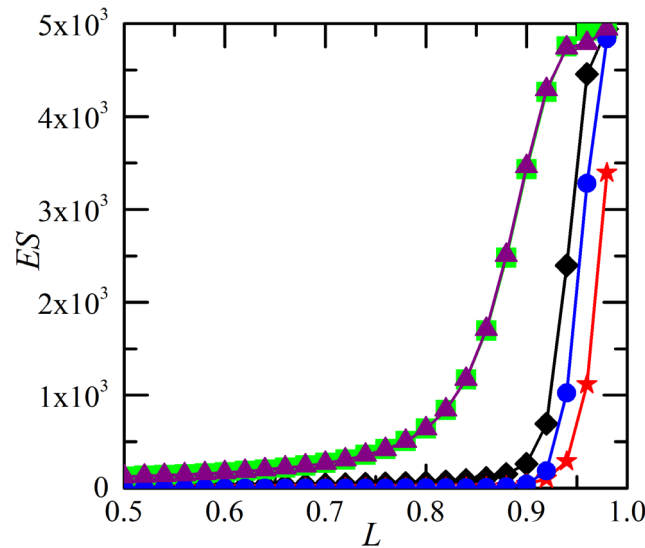
Figure 8. Average avalanche size *ES* as a function of the system loading level *L* in power grid. Results for five different restoration strategies: (1) $p_r=0$ (black diamonds); (2) $t_r=1$, $p_r=1$, $D_r^{min}=0$, $D_r^{max}=0.1$ (green squares); (3) $t_r=4$, $p_r=1$, $D_r^{min}=0$, $D_r^{max}=0.1$ (purple triangles); (4) $t_r=1$, $p_r=1$, $D_r^{min}=-0.1$, $D_r^{max}=0$ (red stars); (5) $t_r=4$, $p_r=1$, $D_r^{min}=-0.1$, $D_r^{max}=0$ (blue circles). Results are averaged over 1,000 realizations. All components are initially loaded by independent random variables $L_1, L_2, …, L_n$ from Gaussian distribution $N(u_1,\sigma_1^2)$ in [L_{min}, L_{max}], and D_r follows Gaussian distribution $N(u_2,\sigma_2^2)$ in [D_r^{min}, D_r^{max}]. The model parameters are the same in all simulations: $L_{max}=L_{fail}=1$, $u_1=L=(L_{min}+L_{max})/2$, $\sigma_1^2=(L_{max}-L_{min})^2/12$, $D=0.01$, $Q=0.05$, $u_1=(D_r^{min}+D_r^{max})/2$ and $\sigma_2=D_{max}-D_{min}$.

doi:10.1371/journal.pone.0112363.g008

Figure 8 compares different restoration strategies in terms of restoration timing t_r and strength p_r by measuring *ES*. There is a transition of *ES* occurring around critical point $L_c=0.9$ without restoration ($p_r=0$). As shown in Fig. 8, cascading failure under restoration ($p_r>0$) with negative D_r generates smaller *ES* than the case without restoration ($p_r=0$). For negative D_r, early restoration (e.g., $t_r=1$) ends up with more functional components than late restoration (e.g., $t_r=4$). For positive D_r, restoration worsens the system in terms of *ES*. The results are similar to Fig. 1.

Figure 9 further explores the effect of restoration disturbance in terms of the system load fluctuations (*SLF*). We can see the effects of restoration are heavily influenced by the restoration strategies. For subcritical loading ($L=0.8$), *SLF* increases for negative D_r and almost stays constant for positive D_r, while restoration will worsen system for each D_r (Fig. 9b). For supercritical loading ($L=0.95$), *SLF* increases for negative D_r and decreases for positive D_r, while early restoration ($t_r=1$) will improve system for each D_r (Fig. 9d). Restoration can improve system only for certain values of system loading for a given D_r.

Conclusions

Proper restoration during cascading failures can actively prevent failure propagation through the entire network. We have proposed a novel modeling
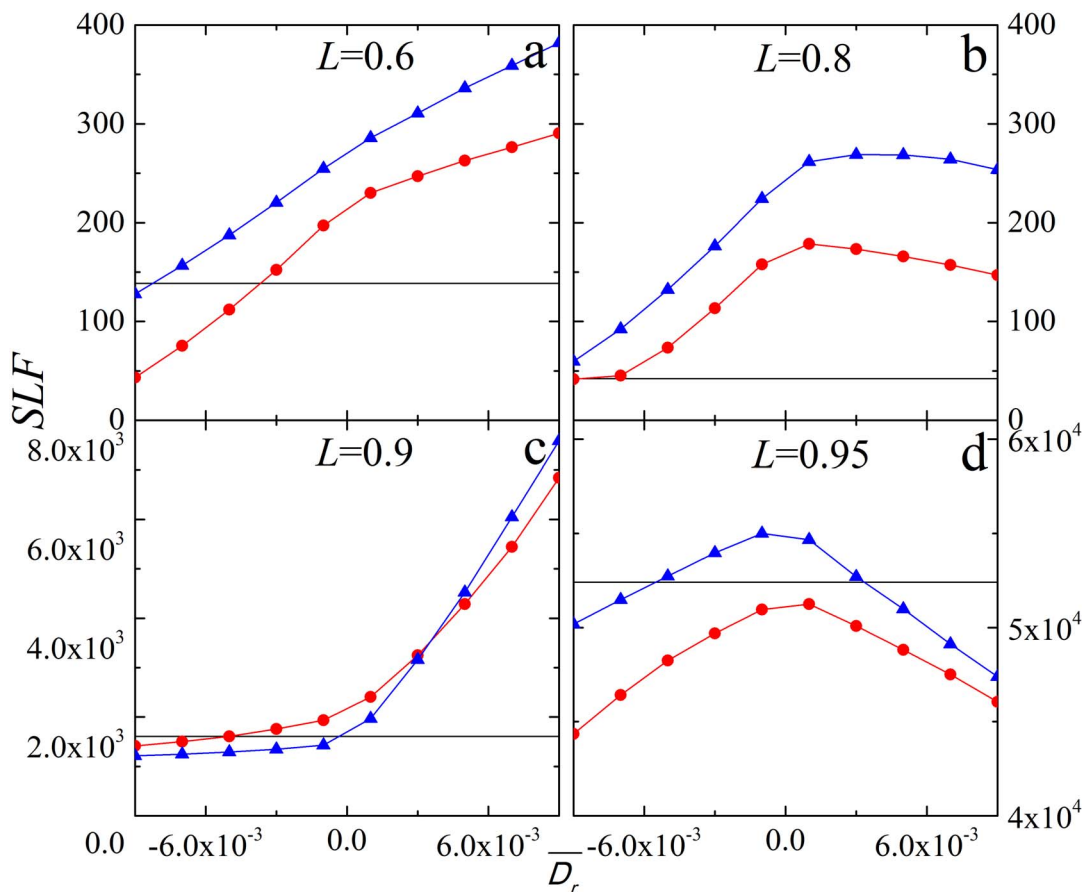
Figure 9. System load fluctuations *SLF* as a function of the average restoration disturbance $\overline{D_r} = u_2$ for different system loading level *L* in power grid. Results for different restoration strategies: (1) $p_r=0$ (black, no symbols); (2) $t_r=1$, $p_r=1$ (red circles); (3) $t_r=4$, $p_r=1$ (blue triangles). Here we set $D_r^{max} - D_r^{min} = 2 \times 10^{-3}$. The other parameters are the same as in Fig. 8.

framework to investigate restoration effect during cascading failures with respect to restoration timing t_r and strength p_r. The model also considers additional disturbances on the system due to the restoration actions themselves. The effects of the restoration have been analyzed with respect to the mean number of failed components *ES* and the system load fluctuations *SLF*. *ES* focuses on the final state of the cascade-restoration process, whereas the newly introduced measure *SLF* describes the dynamical behavior of the systems.

By applying the proposed modeling framework on the example system, we find that the restoration effects also depend on the combination of system loading level *L* and restoration disturbance D_r. Although the system can be improved by proper in-process restoration, the application of restoration should be implemented carefully considering the system loading level. Our framework and findings can help to evaluate restoration scheme of complex systems and provide insights into the development of optimal restoration strategy against cascading failures, which

are helpful for guiding improvements of reliability and robustness of actual network systems.

Given the rapid development of Micro-Grid technology, it is interesting and necessary to study the restoration for Micro-Grid against cascading failures. Although, for now we have no data for the Micro-Grid, we will perform the relevant study in the future based on the framework provided in this paper. Based on our framework provided in the paper, more realistic scenario considering system real-time status can also be studied in the near future.

Acknowledgments

Author Contributions

Derivation of the formula: CL DL EZ RK. Conceived and designed the experiments: DL RK EZ. Performed the experiments: CL DL. Analyzed the data: CL DL EZ RK. Contributed reagents/materials/analysis tools: CL DL EZ RK. Contributed to the writing of the manuscript: CL DL EZ RK.

References

1. **Watts DJ** (2002) A simple model of global cascades on random networks. Proc Natl Acad Sci USA 99: 5766–5771.

2. **Kröger W, Zio E** (2011) Vulnerable systems. London: Springer.

3. **Lee KM, Yang JS, Kim G, Lee J, Goh KI, et al.** (2011) Impact of the topology of global macroeconomic network on the spreading of economic crises. PloS one 6: e18443.

4. **Buldyrev SV, Parshani R, Paul G, Stanley HE, Havlin S** (2010) Catastrophic cascade of failures in interdependent networks. Nature 464: 1025–1028.

5. **Barrett C, Channakeshava K, Huang F, Kim J, Marathe A, et al.** (2012) Human initiated cascading failures in societal infrastructures. PloS one 7: e45406.

6. **Dobson I, Carreras BA, Lynch VE, Newman DE** (2007) Complex systems analysis of series of blackouts: Cascading failure, critical points, and self-organization. Chaos 17: 026103.

7. **Boccaletti S, Bianconi G, Criado R, del Genio CI, Gómez-Gardeñes J, et al.** (2014) The structure and dynamics of multilayer networks. Physics Reports. DOI: 10.1016/j.physrep.2014.07.001.

8. **Atputharajah A, Saha TK** (2009) Power system blackouts-literature review. In: Proc Int Conf Industrial and Information Systems (ICIIS). 460–465.

9. **Weng X, Hong Y, Xue A, Mei S** (2006) Failure analysis on China power grid based on power law. Journal of Control Theory and Applications 4: 235–238.

10. **Balderer C, Guarisco M, Laumanns M, Zenklusen R** (2009) Repair strategies for minimising the risk of cascading failures in electricity networks. Int J Critical Infrastructures 5: 51–71.

11. **Francis R, Bekera B** (2014) A metric and frameworks for resilience analysis of engineered and infrastructure systems. Rel Eng Syst Safety 121: 90–103.

12. **Asztalos A, Sreenivasan S, Szymanski BK, Korniss G** (2014) Cascading failures in spatially-embedded random networks. PloS one 9: e84563.

13. **Caballero Morales SO** (2013) Economic Statistical Design of Integrated X-bar-S Control Chart with Preventive Maintenance and General Failure Distribution. PloS one 8: e59039.

14. **Albert R, Jeong H, Barabási AL** (2000) Error and attack tolerance of complex networks. Nature 406: 378–382.

15. **Gutfraind A** (2010) Optimizing topological cascade resilience based on the structure of terrorist networks. PloS one 5: e13448.

16. **Jin Q, Wang L, Xia CY, Wang Z** (2014) Spontaneous symmetry breaking in interdependent networked game. Scientific reports 4: 4095.

17. **Liu C, Du WB, Wang WX** (2014) Particle Swarm Optimization with Scale-Free Interactions. PloS one 9: e97822.

18. **Du WB, Wu ZX, Cai KQ** (2013) Effective usage of shortest paths promotes transportation efficiency on scale-free networks. Physica A 392: 3505–3512.

19. **Motter AE, Lai YC** (2002) Cascade-based attacks on complex networks. Phys Rev E 66: 065102.

20. **Shuang Q, Zhang M, Yuan Y** (2014) Performance and Reliability Analysis of Water Distribution Systems under Cascading Failures and the Identification of Crucial Pipes. PloS one 9: e88445.

21. **Helbing D** (2013) Globally networked risks and how to respond. Nature 497: 51–59.

22. **Cadini F, Zio E, Petrescu C** (2010) Optimal expansion of an existing electrical power transmission network by multi-objective genetic algorithms. Rel Eng Syst Safety 95: 173–181.

23. **Ren H, Dobson I, Carreras BA** (2008) Long-term effect of the n-1 criterion on cascading line outages in an evolving power transmission grid. Power Systems, IEEE Transactions on 23: 1217–1225.

24. **Talukdar SN, Apt J, Ilic M, Lave LB, Morgan MG** (2003) Cascading failures: survival versus prevention. Elect J 16: 25–31.

25. **Peças Lopes JA, Moreira CL, Resende FO** (2005) Microgrids black start and islanded operation. In: Proc 15th PSCC.

26. **Moreira CL, Resende FO, Peças Lopes JA** (2007) Using low voltage microgrids for service restoration. Power Systems, IEEE Transactions on 22: 395–403.

27. **Yadav G, Babu S** (2012) NEXCADE: Perturbation Analysis for Complex Networks. PloS one 7: e41827.

28. **Quattrociocchi W, Caldarelli G, Scala A** (2014) Self-healing networks: redundancy and structure. PloS one 9: e87986.

29. **Adibi M, Clelland P, Fink L, Happ H, Kafka R, et al.** (1987) Power system restoration-a task force report. Power Systems, IEEE Transactions on 2: 271–277.

30. **Adibi MM, Borkoski JN, Kafka RJ** (1987) Power system restoration-the second task force report. Power Systems, IEEE Transactions on 2: 927–932.

31. **Zio E, Golea LR, Sansavini G** (2012) Optimizing protections against cascades in network systems: A modified binary differential evolution algorithm. Rel Eng Syst Safety 103: 72–83.

32. **Zio E, Golea LR, Sansavini G** (2011) Optimization of electrical grid protection by a differential evolution algorithm. In: Proc Eur Safety Rel Conf (ESREL 2011). 2515–2521.

33. **Adibi MM, Martins N** (2008) Power system restoration dynamics issues," In: Proc IEEE PES General Meeting. 1–8.

34. **Fink LH, Liou KL, Liu CC** (1995) From generic restoration actions to specific restoration strategies. Power Systems, IEEE Transactions on 10: 745–752.

35. **Adibi MM, Fink LH** (2006) Overcoming restoration challenges associated with major power system disturbances-Restoration from cascading failures. IEEE Power Energy Mag 4: 68–77.

36. **Henderson M, Rappold E, Feltes J, Grande-Moran C, Durbak D, et al.** (2012) Addressing restoration issues for the ISO New England system. In: Proc IEEE PES General Meeting. 1–5.

37. **Vaiman M, Hines P, Jiang J, Norris S, Papic M, et al.** (2013) Mitigation and prevention of cascading outages: Methodologies and practical applications. In: Proc IEEE PES General Meeting. 1–5.

38. **Koch S, Chatzivasileiadis S, Vrakopoulou M, Andersson G** (2010) Mitigation of cascading failures by real-time controlled islanding and graceful load shedding. In: Proc IREP Symposium–Bulk Power System Dynamics and Control–VIII. 1–19.

39. **Ahsan MQ, Chowdhury AH, Ahmed SS, Bhuyan IH, Haque MA, et al.** (2012) Technique to Develop Auto Load Shedding and Islanding Scheme to Prevent Power System Blackout. Power Systems, IEEE Transactions on 27: 198–205.

40. **Zima M, Andersson G** (2004) Wide area monitoring and control as a tool for mitigation of cascading failures. In: Proc Int Conf Probabilistic Methods Applied to Power Systems. 663–669.

41. **Zhang N, Kezunovic M** (2006) Improving real-time fault analysis and validating relay operations to prevent or mitigate cascading blackouts. In: Proc IEEE PES Transm Distrib Conf. 847–852.

42. **Cohen R, Havlin S** (2010) Complex networks: Structure, Robustness and Function. Cambridge. England: Cambridge University Press.

43. **Dobson I, Chen J, Thorp JS, Carreras BA, Newman DE** (2002) Examining criticality of blackouts in power system models with cascading events. In: Proc 35th Hawaii Int Conf Syst Sci. 10.

44. **Dobson I, Carreras BA, Newman DE** (2005) A loading-dependent model of probabilistic cascading failure. Probab Eng Inf Sci 19: 15–32.

45. **Dobson I, Carreras BA, Newman DE** (2004) A branching process approximation to cascading load-dependent system failure. In: Proc 37th Hawaii Int Conf Syst Sci. 10.

46. **Watts DJ, Strogatz SH** (1998) Collective dynamics of 'small-world' networks. Nature 393: 440–442.